ELSEVIER

PII: S0032-3861(96)00787-2

Polymer Vol. 38 No. 10, pp. 2329–2335, 1997

0032-3861/97/$17.00 + 0.00

The visualization of spatial gradients in polymer and solvent dynamics for mixed solvents ingressing poly(methyl methacrylate) using stray field magnetic resonance imaging

D. M. Lane and P. J. McDonald*
Department of Physics, University of Surrey, Guildford, Surrey GU2 5XH, UK
(Received 16 April 1996; revised 12 June 1996)

Stray-field magnetic resonance imaging (m.r.i.) has been used to study the ingress of methanol and methanol–acetone vapour mixtures into poly(methyl methacrylate), PMMA. For pure methanol, the polymer concentration and ^{1}H spin–spin relaxation time is found to be constant across the swollen region. The relaxation time is, however, greater by a factor of 1.1 compared to the rigid polymer. For mixed solvents, the polymer chain spin–spin relaxation time is greater by factors ranging from 1.1 to 1.4 across the swollen region in samples exposed to solvent for up to 1 week, providing evidence for a spatial gradient in the polymer chain dynamics. Small polymer concentration gradients are also seen in samples exposed to methanol–acetone mixtures. In further experiments, stray field imaging and gradient spin echo diffusion techniques have been combined for the first time in order to make high spatial resolution measurements of the solvent self-diffusion coefficient. These experiments yield complementary spatial gradients in the diffusion coefficient such that the diffusion coefficient typically varies by a factor of 2 across any one sample, ranging from 0.15 to 0.30 $\times 10^{-6}$ cm^2 s^{-1} over 0.8 mm for pure methanol in PMMA and from 1.8 to 3.2 $\times 10^{-6}$ cm^2 s^{-1} over 1.5 mm for 70% methanol–30% acetone. These results are discussed in the context of previous liquid-state m.r.i. investigations of the solvent alone in similar systems. © 1997 Elsevier Science Ltd.

(Keywords: magnetic resonance imaging; stray field imaging; diffusion)

INTRODUCTION

Nuclear magnetic resonance imaging (m.r.i.) and pulsed field gradient spin echo (p.f.g.s.e.) measurements[1] are making an increasingly important contribution to the study of solvent ingress in polymers. Magnetic resonance imaging is a non-destructive and non-invasive technique which provides spatially resolved measurements of the solvent concentration as a function of time. These concentration profiles are important in testing models of the ingress dynamics, which ranges from generalized Fickian through to case II diffusion[2,3]. The broad range of observed phenomena is a result of complex interaction between the solvent and the polymer. In general, the ingressing solvent swells the polymer. The rate of solvent advance is controlled by the mechanical relaxation of the polymer chains. Fickian diffusion results when the polymer relaxation time is fast compared to the rate of solvent ingress, whereas case II diffusion results when the polymer relaxation time is slow compared to the rate of solvent ingress. Case II diffusion is characterized by an induction period, after which a sharp solvent front advances into the polymer linearly with time. Behind the front the solvent concentration is essentially uniform while ahead of it the concentration is zero. The front itself consists of a very short range Fickian precursor which is not normally resolved in m.r.i. experiments but is observable using ion beam techniques[4]. Measurements of the magnetic resonance spin–spin and spin–lattice relaxation times, T_2 and T_1 respectively, and of self-diffusion coefficients, D, using p.f.g.s.e. techniques, are important for inferring information about the microscopic solvent and polymer chain dynamics. The spin–spin relaxation rate, T_2^{-1}, is proportional to the n.m.r. resonance linewidth. In general, it decreases with increased molecular mobility. In particular, glassy polymers are characterized by broad lines and very short T_2 relaxation times, of an order of microseconds, whereas free solvents are characterized by narrow lines and long T_2 relaxation times, typically seconds. Restricted and/or bound solvents and swollen polymers have intermediate values.

The basic principles by which m.r.i. is used to study solvents in polymers were established by Blackband and Mansfield who visualized the ingress of water into nylon 6.6[5,6]. In common with most subsequent studies, the fluid ingress was monitored over a period of time using conventional m.r.i. microscopy methods which are only sensitive to the mobile (long T_2) components in the sample. Consequently, the nylon remained undetected. This particular example exhibited generalized Fickian diffusion and the authors were able to apply the

*To whom correspondence should be addressed

Boltzmann transformation[2] in order to obtain the water diffusion coefficient as a function of concentration. Other systems which have received considerable attention include elastomers[7,8], polyethylene[9] and poly(vinylchloride)[10], amongst others.

A number of authors have studied solvents ingressing into poly(methyl methacrylate), PMMA, using both n.m.r. and non-n.m.r. techniques. Weisenberger and Koenig studied the ingress of both pure methanol and pure acetone into PMMA[11,12]. Methanol ingressing PMMA, in particular, exhibits case II diffusion. This work was important in that it showed a spatial gradient in the solvent nuclear spin relaxation times, T_1 and T_2, and in the solvent self-diffusion coefficient across the swollen polymer. This implied a gradient in solvent mobility and hence suggested that the solvent–polymer system was evolving long after the case II front had passed and after the local solvent concentration had equilibrated. However, they were unable to observe the swollen polymer. Tabak and Corti[13], on the other hand, specifically did see the polymer in the case of deuterated chloroform ingressing PMMA as well as carbon tetrachloride in polystyrene. In the case of PMMA, they applied the Boltzmann transformation to infer the polymer concentration dependent transport diffusion coefficient of the solvent. However, in the light of possible gradients in relaxation times across the swollen region which affect signal intensity, and the sample swelling which affects the transformation boundary conditions, the validity of this procedure is uncertain. In the case of polystyrene, Tabak and Corti[13] concluded that there was a gradient in the polymer chain mobility across the swollen polymer on the basis of spatially resolved spin-lattice relaxation measurements.

Mareci and Donstrup[14] also studied the swelling of PMMA in the presence of chloroform, using liquid-state m.r.i. methods. They used spin relaxation time contrast and deuterated chloroform to separately visualize both the solvent and the mobilized polymer chains. In a theoretical analysis which accompanied the results, they attempted to relate the observed spin-lattice relaxation rate of the swollen polymer chains to the chain segmental motion on the basis of the semi-phenomenological 'blob' model of de Gennes[15]. Nuclear reaction techniques have been used to study 1,1,1-trichloroethane ingressing PMMA[16]. Finally, Lee[17] has used optical microscopy to study the swelling of PMMA beads immersed in methanol as a function of temperature, while Lee and Fu[18] have used gravimetric methods.

The primary limitation of conventional liquid-state m.r.i. is that, due to a lack of molecular motion, the polymer is either unseen or poorly seen. As already noted, Mareci *et al.* observed the swollen polymer chains of PMMA in chloroform, but in this case the increased chain mobility, and hence T_2, is considerable and indeed their analysis assumes a low polymer concentration. In order to make accurate spatially resolved measurements of polymer and solvent concentrations, or to learn about the polymer chain dynamics at high polymer concentrations, it is necessary to use short T_2, that is broad-line m.r.i. methods which are able to spatially resolve the polymer as well as the liquid. There are now a large number of broad-line techniques which have been extensively reviewed elsewhere[19]. One of these, gradient echo imaging, has recently been applied to solvent ingress in elastomers[20]. However, perhaps the most promising method for high spatial resolution studies of glassy polymers is stray-field imaging[21].

Stray-field imaging (STRAFI) exploits the enormous fringe-field gradient existing around large high-field superconducting magnets. It is beginning to make a significant contribution to magnetic resonance microscopy of several materials systems, including cements and concretes[22,23], soils[24], sodium silicates[25] and polymers[26]. The development of these applications has resulted partly from more widespread appreciation of the general method. It has also resulted from theoretical and experimental advances[27,28]. In the case of polymers[26], stray-field imaging was used to study the ingress of acetone into PVC, which was seen to follow case II diffusion dynamics. The experiment revealed a gradient in the spin–spin relaxation characteristics of the polymer across the swollen region. Evidence was not seen for a solvent relaxation time gradient, although, in the light of subsequent theoretical and technical developments and the nature of the particular measurements made, one may have been present. The fact that the measurements were performed on a moving sample at a relatively long pulse gap would have masked this[27].

At the same time as developments have taken place in stray-field imaging, other authors have been using the fringe-field gradient for the measurement of very slow self-diffusion rates in experiments analogous to the p.f.g.s.e. method. In these experiments diffusion in the field gradient between the two pulses of an echo sequence results in incomplete echo refocusing and hence echo attenuation from which the self-diffusion coefficient is calculated. The first such measurements were reported by Kimmich *et al.*[29,30]. More recently Wu[31] has devised a new pulse sequence which offers some practical advantages for the measurement of very small diffusion coefficients.

EXPERIMENTAL

The stray-field imaging experiment has been described on a number of occasions[21,26,27]. In essence, the sample is placed in the strong field gradient to be found below the central homogeneous-field region of a large superconducting magnet, in this case 9.4 T. This gradient, which is used to spatially separate n.m.r. resonances from different parts of the sample, is several orders of magnitude greater than that normally available from current windings in conventional scanners. It can easily separate broad resonances with high spatial resolution. A short radio-frequency excitation pulse is applied which excites nuclear magnetization in a narrow slice of the sample orthogonal to the field gradient. The amplitude of the excited magnetization is recorded as a measure of the hydrogen (in a ^{1}H experiment) content in that slice. Additionally, the magnetization decay rate is measured in order to infer T_2 and hence elicit molecular dynamic information. For experimental reasons the decay is necessarily recorded in the form of an echo train created by a train of pulses. The sample is moved up through the gradient and the measurement repeated for the next slice. In this way a one-dimensional profile is built up.

The profiles measured here were acquired using the multiple quadrature echo sequence, $90_x-\tau-(90_y-\tau-\text{echo}-\tau)_n$, where 90_x signifies a 90° radio-frequency excitation pulse of relative quadrature phase x and τ is a short time interval, operating on a Chemagnetics Infinity

n.m.r. spectrometer. The pulse length used in this work was typically 10 μs, corresponding to a slice thickness of approximately 50 μm in the 58 T m^{-1} gradient. The ^{1}H n.m.r. frequency was 236 MHz. The pulse gap, τ, was varied from 20 to 400 μs. Each profile presented here is typically the result of 64 averages recorded over 37 minutes. Unlike many realizations of stray-field imaging which use continuous sample motion, the sample was stationary for all of the echo measurements and was moved incrementally between measurements to the next slice. Although slower, this prevented any modulation of echo trains due to sample movement[27].

The PMMA samples used in this work were cylindrical, 6.5 mm in diameter and 4 mm long, and cut from a 5600 mm^2 × 4 mm deep block of material. The initial block was prepared by pressing as received, uncross-linked, PMMA powder (Aldrich Chemical Co.) with a molecular weight of $M_w = 996\,000$ at a temperature of 165°C and a pressure of up to 10 kN cm^{-2}. The block was cooled slowly over a period of 2 h whilst maintaining the pressure. The resulting pressed block was uniformly transparent. It had a density of 1220 kg m^{-3}, comparable to literature values. The glass transition temperature, measured by differential scanning calorimetry analysis, was 109°C, again comparable to literature values. To carry out the STRAFI experiments, the solvent was placed in a ground, flat-bottomed glass tube of 9 mm internal diameter and the sample lightly glued to a PTFE tube stopper. This arrangement created a small vapour volume (<1 cm^3) between the lower sample surface and the liquid solvent in which equilibrium vapour pressure was rapidly established. The samples were profiled in the vertical direction.

Each sample was aligned within the spectrometer to better than ±12 μm across the surface, half the profile spatial resolution, so that the sample edge was well delineated in the profiles at the start of the experiment. However, at later times, the sideways ingress of the solvent into the samples and surface deformation became significant and were observable as rounding of the profiles which integrated across horizontal slices. No simple solution to this problem has yet been found. Three-dimensional imaging is impractical because it is far too slow to record dynamic solvent uptake. All measurements and sample storage were carried out at 21 ± 1°C.

Three experimental regimes have been explored in this work. Firstly, ^{1}H stray-field imaging has been used to follow the absorption of deuterated solvents into PMMA. These experiments, performed using a small pulse gap, have been used to measure the polymer spin–spin relaxation time in both the swollen and the rigid state and to look specifically for spatial gradients in the chain mobility behind the solvent front. Such an observation would complement the gradient in solvent dynamics seen in PMMA by Weisenberger and Koenig[11,12] and our own observation of a gradient in PVC dynamics seen using STRAFI[26]. Secondly, similar short pulse gap experiments have been performed using non-deuterated solvents. These have been used to measure the relative polymer and solvent concentrations across the swollen polymer, measurements which cannot be made by liquid state methods observing the solvent alone. Again, evidence has been sought for spatial gradients. Finally, longer pulse gap experiments have been performed. From these experiments it has been possible to infer the solvent self-diffusion coefficient in the polymer matrix as a function of acetone–methanol concentration. This is the first time that stray-field imaging has been combined with stray-field diffusion measurements in one experiment. Throughout the study mixtures of acetone and methanol have been used, as this provides a more gradual change in parameters than simply changing the solvent from methanol to acetone to chloroform etc. Mixed solvent ingress has previously been studied for polycarbonate[32] and elastomeric[33] systems.

STRAFI AND DIFFUSION: THEORY

It is well known that for a mobile system, in the presence of magnetic field gradients between the pulses, and for the more usual Carr–Purcell–Meiboom–Gill multiple spin echo sequence, defined by $90_x-\tau-(-180_y-\tau$ echo$-\tau)_n$, the echo intensities decay according to

$$M(2n\tau) = M(0)\exp\left(-\frac{2n\tau}{T_2} - 2k\gamma^2g^2n\tau^3D\right)$$
$$= M(0)\exp\left(-\frac{2n\tau}{T_2^{obs}}\right) \quad (1)$$

where

$$\frac{1}{T_2^{obs}} = \frac{1}{T_2} + k\gamma^2g^2\tau^2D \quad (2)$$

In these expressions, T_2 is the true spin–spin relaxation time and T_2^{obs} is the observed value, γ is the magnetogyric ratio, g is the gradient strength, τ is the pulse gap, n the echo number, D the self-diffusion coefficient and k a constant, in this case equal to 1/3. By making τ arbitrarily small it is always possible to measure T_2 even in the presence of a gradient. Extrapolating the decay curve back to time zero provides a reliable measure of the initial magnetization $M(0)$ and hence, in a ^{1}H experiment, hydrogen density. On the other hand, large values of τ permit D to be accurately measured, one method being to plot $1/T_2^{obs}$ against τ^2, for which the gradient is $k\gamma^2g^2D$.

Other pulse sequences can be used to measure diffusion, for instance the stimulated echo sequence, $90_x-\tau_1-90_x-\tau_2-90_x-\tau_1$ echo, with the gradients applied during the τ_1 intervals. For this sequence, with $\tau_1 = \tau_2$ and $n = 1$, the constant $k = 5/6$. Stimulated echo sequences differ from spin echo sequences in that the magnetization spends part of the measurement period aligned along the z (longitudinal) direction. With spin echo sequences the magnetization remains in the xy (transverse) plane throughout the measurement period. STRAFI is additionally complicated. Since the gradient is of necessity present during the pulses, the pulses generate imperfect rotations and the sample is, for the most part, off resonance. Hence some, but not all, of the magnetization spends part of the time along the z direction during a STRAFI experiment. In consequence, echoes are a mix of normal spin echoes and stimulated echoes. Echo intensity correction factors in the absence of diffusion are known for both stationary samples and samples moving at constant velocity[27]. For a stationary sample the first echo intensity must be multiplied by 1.5. A similar correction to the constant k must be made when diffusion is measured. However, the magnitude of

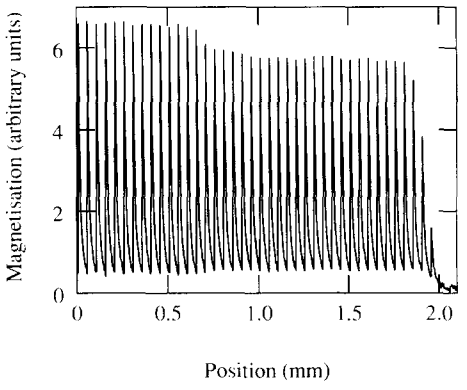

Figure 1 A stray field ^{1}H profile of a PMMA sample exposed to deuterated methanol vapour for 163 h from the right. The main ^{1}H concentration profile consists of the peaks at 50 μm intervals and referenced to the millimetre scale. Each peak is composed of a T_2 decay curve built from the intensities of 16 echoes acquired with a pulse gap τ of 20 μs. Each decay is therefore $2 \times 16 \times 20 = 640$ μs long. In every case the first echo has been multiplied by 1.5

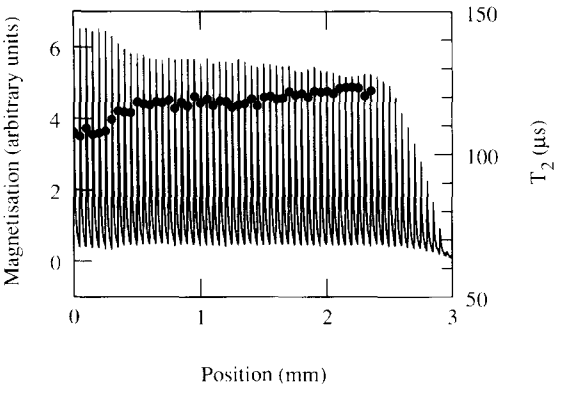

Figure 2 A similar profile to that in *Figure 1* except that the solvent is 80 wt% deuterated methanol and 20% deuterated acetone. The profile was acquired after 166 h sample exposure. The discrete points, referred to the right-hand scale, show the polymer chain spin relaxation time calculated at each location from the echo trains

k is as yet unknown for the extreme case of STRAFI with the quadrature echo sequence. In consequence, k has been measured empirically by calculation from the decay rate of echoes obtained from bulk water, for which the self-diffusion coefficient at 21°C is 2.3×10^{-5} cm^2 s^{-1} [34]. As a double check, some measurements have also been made using only first echo data with multiple pulse gaps. First echoes are pure spin echoes. For the quadrature sequence and parameters used in this work, $k = 0.55$.

RESULTS AND DISCUSSION

Figure 1 shows ^{1}H data recorded from a PMMA sample exposed to deuterated methanol for 163 h. The use of deuterated methanol renders the solvent unseen in this profile and so all the signal intensity is due to the hydrogen within the polymer. The figure shows magnetization recorded as a function of both position and time collapsed onto a single axis which, for convenience, is labelled by position only. The main ^{1}H concentration profile is composed of the peaks which occur with a spatial resolution of 50 μm. At each spatial step, a multiple echo train of 16 echoes has been recorded using a pulse gap, τ, of 20 μs. The echo intensity decays are shown following the peaks. Each decay is $2 \times 20 \times 16 = 640$ μs long. In each case the first echo has been multiplied by 1.5, as discussed above. The solvent ingresses from the right. The initial position of the exposed polymer surface is at 1.75 mm on the trace. Hence the signal seen beyond this is due to swelling. The solvent front is at 0.60 mm. Observation of a series of profiles recorded at different times shows that this front progresses across the sample linearly with time, as previously reported and as expected of a case II diffusion system. The profile intensity is about 10% less in the imbibed region, due to the polymer swelling which reduces the local polymer density. To support this assertion, we note that the magnetization intensity integrated over the whole sample remains constant with time. The polymer spin–spin relaxation time, T_2, has been measured at each location across the profile by fitting a single-component exponential decay to each echo train. In the rigid, unswollen polymer it is found to be equal to 106 μs and is, as expected, constant. This value is greater than that normally found for rigid polymers, more typical values being 5–25 μs, because the quadrature echo sequence introduces some degree of line narrowing and further because the multiecho version used with small τ approximates to a spin locking sequence, so weighting the relaxation time towards $T_{1\rho}$, the spin-lattice relaxation time in the rotating reference frame. In the swollen region the polymer relaxation time is 114 μs, some 7.5% greater than the rigid polymer value. Importantly, as far as this study is concerned, it is constant across the swollen region and does not exhibit a spatial gradient. This is surprising, given the gradient in the solvent relaxation time reported by Weisenberger and Koenig[11,12]. The increase in polymer relaxation time in the swollen region compared to the rigid polymer is attributed to the increased mobility of the polymer chains resulting from the solvent ingress and swelling.

Figure 2 shows the results of a similar experiment using a solvent mixture of 80 wt% deuterated methanol and 20% deuterated acetone, equivalent to 0.876 mole fraction of methanol. The profile shown was recorded after 166 h and is displayed in a similar manner to *Figure 1*. The original polymer surface is at 2.4 mm on the trace and the front position is at 0.30 mm. In this case there is a small, but definite, gradient in the polymer density across the swollen region of the sample which is accounted for only in part by rounding (uneven swelling) of the polymer surface. It is thus concluded that there is greater swelling near the exposed surface than near the solvent front. The discrete data points in the figure represent the polymer spin–spin relaxation time calculated from the echo trains in the profile and are referenced to the right-hand scale. A gradient in the polymer spin relaxation time across the swollen region is observed, with the longest time being recorded near the sample surface. The polymer relaxation time is 122 μs on the exposed surface and 115 μs close to the solvent front. The rigid polymer relaxation time is again 106 μs.

At this stage no adequate models exist to make a quantitative link between the relaxation time and the degree of swelling. Attempts to adapt the model proposed by Mareci and Donstrup[14] to the measurements made here have so far proved unsuccessful. The model is seemingly only appropriate for polymers with a much higher degree of swelling than occurs here. There are, however, a number of features which any future model must adequately explain. Careful inspection of

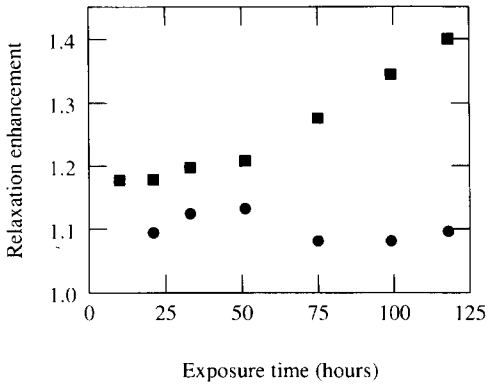

Figure 3 The PMMA chain spin–spin relaxation time enhancement (as defined in the text), measured at the surface (squares) and solvent front (circles) of a sample exposed to a mixture of 70% deuterated methanol and 30% deuterated acetone, as a function of exposure time

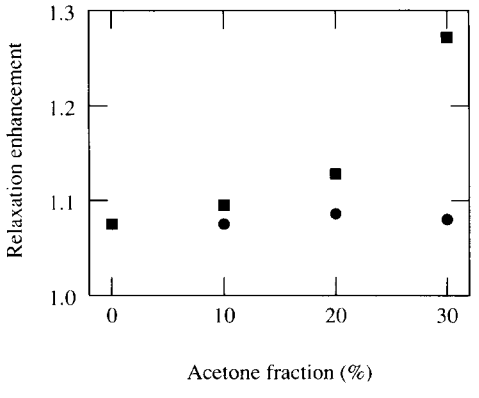

Figure 4 The PMMA chain spin–spin relaxation time enhancement (as defined in the text), measured at the surface (squares) and solvent front (circles) of a series of samples exposed to different deuterated methanol–acetone mixture ratios for 72 ± 3 h

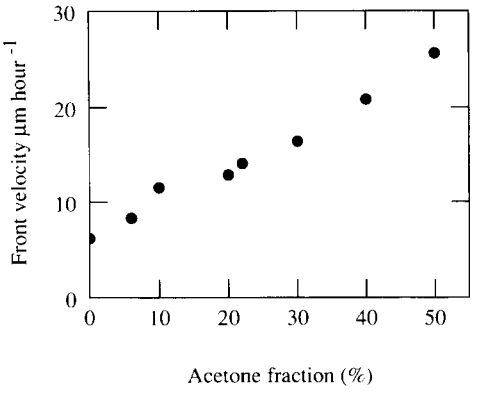

Figure 5 The solvent front velocity measured from stray-field profiles and defined relative to the original sample surface position, as a function of the acetone fraction in the solvent

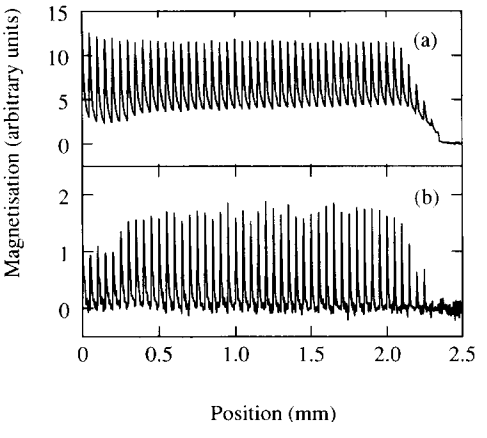

Figure 6 Stray-field profiles, displayed similarly to those in *Figure 1*, of a PMMA sample exposed to a mixture of 94% methanol and 6% acetone for 169 h (a) using a pulse gap of 20 μs; and (b) using a pulse gap of 350 μs. In (a) both the solvent and polymer are visualized, whereas in (b) the polymer is suppressed, leaving only the solvent

profiles recorded from the same sample at different times reveals that the polymer relaxation time at any given location behind the front depends primarily on the length of time for which that part of the polymer has been exposed to the solvent; that is, how far behind the solvent front it is. This seems true in spite of difficulties in the interpretation of profiles of samples exposed to solvent for long periods, or exposed to solvent with a high acetone fraction, in which ingress of the solvent from the sides of the sample, rather than its end face, and also non-uniform surface swelling, cause profile rounding. The relaxation enhancement, defined as the spin–spin relaxation time in the swollen region divided by relaxation time in the rigid polymer, has been calculated at a position close to the sample surface and also near the diffusion front for a number of profiles. This ratio is relatively insensitive to the details of the measurement procedure, and, at the surface, is also insensitive to side ingress and surface rounding. Taken together, these enhancement factors provide a measure of the relaxation time gradients across different samples.

Figure 3 shows how the relaxation enhancement increases with time at the surface of a sample exposed to a 70% methanol and 30% acetone mixture. The figure also shows how the ratio remains approximately constant close to the solvent front. Likewise, *Figure 4* shows the enhancement of the relaxation time after 72 h at the exposed surface and at the solvent front for samples exposed to different methanol–acetone vapour ratios. As might be expected, the surface relaxation enhancement increases with acetone fraction. The solvent front velocity also increases with acetone fraction, as is shown in *Figure 5*, the velocity having been measured from a range of samples exposed to deuterated and non-deuterated solvents. From *Figure 5* it is concluded that, at least for small acetone fractions, the front velocity depends linearly on acetone fraction according to $v = 6.3 + 0.37 f_a$ where v is the velocity in $\mu m\, h^{-1}$ and f_a is the acetone fraction.

Figures 6a and *b* show profiles, in the manner of *Figure 1*, recorded from a sample exposed to a mixture of non-deuterated 94% methanol and 6% acetone for 169 h and for two different pulse gaps, τ, of 20 and 350 μs respectively, both using 16 echo trains. Thus, in *Figure 6a*, the decays at each location extend over 640 μs and, in *Figure 6b*, over 11.2 ms. At short pulse gaps, each of the echo decay trains is a two-component exponential. With a 20 μs pulse gap it is particularly easy to distinguish these two components both quantitatively and qualitatively. The shorter T_2 component is due to the polymer as before, and exhibits all the above characteristics. It decays away to near zero during the course of each echo train. The longer component, on the other

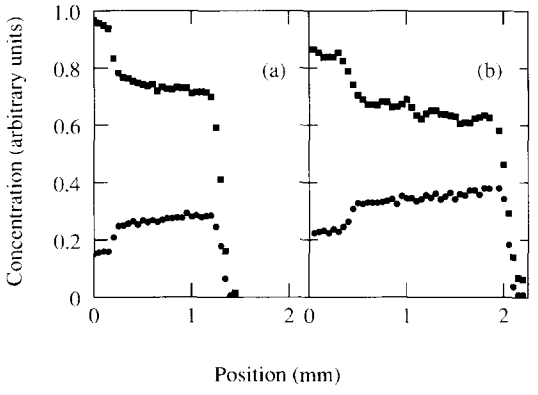

Figure 7 Polymer (squares) and solvent (circles) concentrations calculated from short pulse gap profiles of PMMA samples exposed (a) for 73 h to 94% methanol and 6% acetone; and (b) for 76 h to 78% methanol and 22% acetone

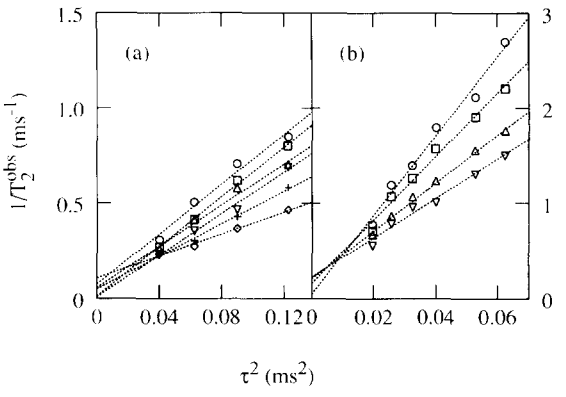

Figure 8 The observed spin–spin relaxation rate as a function of pulse gap for PMMA samples exposed (a) to 94% methanol and 6% acetone for 73 h and shown at 200 μm intervals (circles, squares, triangles, inverted triangles, crosses and diamonds) across the swollen polymer; and (b) exposed to 70% methanol and 30% acetone for 76 h and shown at 300 μm intervals across the swollen polymer. The dotted lines are least squares fits to the data

hand, is due to the solvent and does not decay significantly. Thus, to a first approximation, the profile defined by the first echo intensities is a measure of the combined solvent and polymer density, while the profile defined by the last echo reflects only the solvent. The relative concentrations have been more accurately calculated by fitting each short pulse gap echo train to a two-component exponential decay. Whilst the longer T_2 value is poorly defined, with only a few echoes at short gap, the intensity of the longer component and the T_2 value and intensity of the short component can be reliably calculated. No correction has been made for the relative hydrogen density in the polymer compared to the solvent since the two densities are the same to within 2% for the two separate materials.

The calculated polymer and solvent concentration profiles for the shorter time of 73 h are shown in *Figure 7a*. A slight gradient in the polymer concentration is seen, consistent with the deuterated solvent results, together with a complementary reversed gradient in the solvent concentration. The fact that the solvent fraction is not zero ahead of the front is because ingress of the solvent into the sides of the sample has occurred to a significant extent in this region. *Figure 7b* shows separate polymer and solvent concentration profiles for a second sample, in this case exposed to a mixture of 78% methanol and 22% acetone for 76 h. The main difference is that the relative solvent fraction in the swollen region and the concentration gradients are enhanced.

The relaxation time of the solvent is best measured using larger pulse gaps. An example profile from which this can be done has already been shown in *Figure 6b*. A spatial gradient in the solvent relaxation time is generally observed across each sample, with longer relaxation times being observed nearer to the solvent front. This is in the reverse direction to the gradient observed by Weisenberger and Koenig[11,12]. However, at all locations, and for all solvent mixtures including pure methanol, the relaxation time is found to be dependent on pulse gap, varying at $1/\tau^2$. This is indicative of diffusion through the magnetic field gradient enhancing the relaxation rate and so, as will be seen, our results do not contradict those of Weisenberger and Koenig.

Figure 8a shows the observed relaxation rate, $1/T_2^{obs}$, as a function of τ^2, calculated at 200 μm intervals across profiles recorded with different pulse gaps from the sample exposed to a 94% methanol and 6% acetone

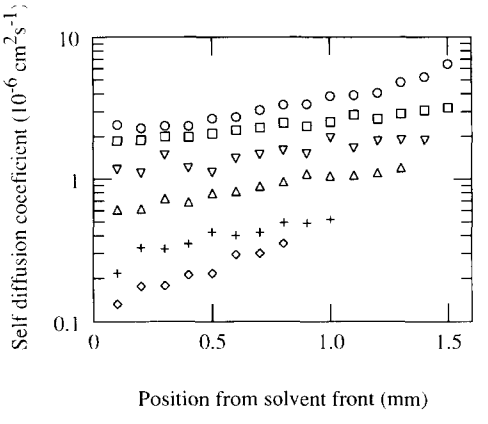

Figure 9 The solvent self-diffusion coefficient, evaluated as described in the text, as a function of position across the swollen polymer, for a series of samples exposed for 73 ± 3 h to pure methanol (diamonds) and methanol–acetone mixtures with 94% (crosses), 85% (triangles), 78% (inverted triangles), 70% (squares) and 60% (circles) methanol. In each case the plot is such that the solvent front is at 0 mm on the scale

mixture for 73 h; in *Figure 8b*, the relaxation rate is calculated at 300 μm intervals across profiles recorded from a sample exposed to 70% methanol and 30% acetone for 76 h. The gradient of these plots is proportional to the local solvent self-diffusion coefficient, D, as explained above. *Figure 9* shows the spatial variation of D for a range of solvent mixtures. This figure makes clear the way in which the diffusion coefficient generally increases with acetone fraction in the solvent. It also shows, in each case, a spatial gradient, with D increasing towards the sample surface.

The vertical intercept of the $1/T_2^{obs}$ vs τ^2 plots provides a measure of $1/T_2$, the true relaxation rate in the absence of diffusion. Careful inspection of *Figure 8b* shows that the region of the sample with the largest gradient (near the surface) also has the longest true T_2 value (smallest $1/T_2$) and that the true T_2 decreases towards the solvent front, in accordance with Weisenberger and Koenig's[11,12] results. A similar though less clear-cut trend is also seen in *Figure 8a*, although in both cases the data quality is too poor to be totally convincing. Nonetheless, the true solvent T_2 values of typically

10 ms are very reasonable and in broad agreement with those of Weisenberger and Koenig.

In conclusion, we note that we have made the first direct, spatially resolved measurements of polymer nuclear spin relaxation times in PMMA exposed to vapours of methanol and methanol–acetone mixtures. Observations of both the polymer and the solvent using STRAFI have permitted the relative concentrations of each to be spatially resolved. We have also made spatially resolved measurements of the solvent self-diffusion coefficient using STRAFI, not previously reported for any materials system. For the ingress of pure methanol, we have not found a spatial gradient in either the polymer spin relaxation time or the extent of swelling for samples exposed for up to 5 days. We have, however, found gradients in both the polymer spin relaxation time and the solvent diffusion coefficient for samples exposed to methanol and acetone mixtures and also, for these samples, a small gradient in the polymer fraction across the swollen region. The gradients generally increase with acetone fraction.

ACKNOWLEDGEMENTS

The authors thank Drs R. A. L. Jones and I. Hopkinson of the Cavendish Laboratory, University of Cambridge, for help with sample preparation, characterization and useful discussions. DML acknowledges a UK Engineering and Physical Sciences Research Council Studentship.

REFERENCES

1. Callaghan, P., *Principles of Nuclear Magnetic Resonance, Microscopy*. Oxford University Press, Oxford, 1991.
2. Crank, J., *The Mathematics of Diffusion*, 2nd Edn, Oxford University Press, Oxford, 1975.
3. Thomas, N. L. and Windle, A. H., *Polymer* 1982, **23**, 529.
4. Lasky, R. C., Kramer, E. J. and Hui, C.-Y., *Polymer* 1988, **29**, 673.
5. Blackband, S. and Mansfield, P., *J. Phys. C: Solid State Phys.* 1986, **19**, L49.
6. Mansfield, P., Bowtell, R. and Blackband, S., *J. Magn. Reson.* 1992, **99**, 507.
7. Webb, A.G. and Hall, L.D., *Polym. Commun.* 1990, **31**, 422.
8. Chang, C. and Komoroski, R.A., *Macromolecules* 1989, **22**, 600.
9. Hyde, T. M., Gladden, L. F., Mackley, M. R. and Gao, P., *J. Polym. Sci.: Part A: Polym. Chem.* 1995, **33**, 1795.
10. Maffei, P., Kiene, L. and Canet, D., *Macromolecules* 1992, **25**, 7114.
11. Weisenberger, L. A. and Koenig, J. L., *Macromolecules* 1990, **23**, 2445.
12. Weisenberger, L. A. and Koenig, J. L., *Macromolecules* 1990, **23**, 2454.
13. Tabak, F. and Corti, M., *J. Chem. Phys.* 1990, **92**, 2673.
14. Mareci, T. H. and Donstrup, S., *J. Mol. Liquids* 1988, **38**, 185.
15. de Gennes, P. G. *Scaling Concepts in Polymer Physics*, Cornell University, Ithaca, 1979.
16. Mills, P. J., Palmstrom, C. J. and Kramer, E. J., *J. Mat. Sci.* 1986, **21**, 1479.
17. Lee, P. I., *Polymer* 1993, **34** (11) 2397.
18. Lee, S. and Fu, T. M., *Polymer* 1995, **36**, 3975.
19. Jezzard, P., Attard, J. J., Carpenter, T. A. and Hall, L. D., *Prog. NMR Spectrosc.* 1991, **23**, 1.
20. Halse, M. R., Rahman, H. J. and Strange, J. H., *Physica B* 1994, **203**, 169.
21. Samoilenko, A. A., Artemov, Yu. D. and Sibel'dina, L. A., *JETP Lett.* 1988, **47**, 348.
22. Black, S., Lane, D. M., McDonald, P. J., Hannant, D. J. and Mulheron, M., *J. Mat. Sci. Lett.* 1995, **14**, 1175.
23. Nunes, T., Randall, E. W., Samoilenko, A. A., Boclart, P. and Feio, G., *J. Phys. D (Appl. Phys.)* 1996, **29**, 805.
24. Kinchesh, P., Randall, E. W. and Zick, K., *Magn. Reson. Imag.* 1994, **12**, 305.
25. Hughes, P. D. M., McDonald, P. J., Rhodes, N. P., Rockliffe, J. W., Smith, E. G. and Wills, J., *J. Colloid Interface Sci.* 1996, **177**, 208.
26. Perry, K. L., McDonald, P. J., Randall, E. W. and Zick, K., *Polymer* 1994, **35**, 2744.
27. Benson, T. B. and McDonald, P. J., *J. Magn. Reson.* 1995, **A112**, 17.
28. Randall, E. W., Samoilenko, A. A. and Nunes, T., *J. Magn. Reson.* 1995, **A116**, 259.
29. Kimmich, R., Unrath, W., Schnur, G. and Rommel, E., *J. Magn. Reson.* 1991, **91**, 136.
30. Kimmich, R. and Fischer, E., *J Magn. Reson.* 1994, **106**, 229.
31. Wu, D., *J. Magn. Reson.* 1995, **A116**, 135.
32. Grinsted, R. A. and Koenig, J. L., *Macromolecules* 1992, **25**, 1229.
33. Webb, A. G. and Hall, L. D., *Polym. Commun.* 1990, **31**, 425.
34. Krynicki, K., Green, C. D. and Sawyer, D. W., *Faraday Discuss. Chem. Soc.* 1978, **66**, 199.